Acetone Photolysis: Kinetic Studies in a Flow Reactor

TAKESHI MATSUURA, A. E. CASSANO, and J. M. SMITH

University of California, Davis, California

The photodecomposition of acetone vapor was studied in a tubular flow, differential reactor at atmospheric pressure and from 82 to 112°C. The products included significant amounts of biacetyl along with carbon monoxide and ethane. A rate equation was developed from a sequence of elementary reactions believed to explain the photolysis of acetone. The effects of light intensity and acetone concentration, indicated in the derived rate equation, were confirmed by the data.

The rate is less than first-order with respect to acetone, and this is believed to be due to reformation of stable acetone molecules by deactivation of CH_3COCH_3*.

Increasing interest in the photoreaction route for commercial production of important chemicals has established a need for rational reactor design procedures. The starting point is a knowledge of the reaction rate as a function of the pertinent variables, which for a gaseous system are temperature, concentrations, wave length, and light intensity. Quantitative values for kinetic constants for photochemical reactions are meager, particularly those derived from measurements in flow reactors which could be used most confidently for scaleup. Huff and Walker (*9*) made kinetic studies of the vapor phase photochlorination of chloroform, and Dranoff and colleagues (*10, 11*) have studied various aspects of the scaleup problem by using data on the liquid phase (aqueous solution) photodecomposition of chloroplatinic acid. Cassano and Smith (*3*) determined rate equations for the gaseous photochlorination of propane. Photochlorination of hydrocarbons occurs by a chain mechanism. This complicates the kinetics by introducing the possibility of heterogeneous termination steps on the reactor wall and attendant diffusion effects. The study reported here refers to the photolysis of acetone, which is a nonchain reaction but still of complex kinetics with multiple products. At the acetone partial pressures used (30 to 220 mm. Hg.) wall effects are reported to be unimportant (*4*). Hence, different and simpler scaleup problems would be expected for this system, in comparison with those for chlorinations.

The objective was a rate equation for acetone photolysis in the gas phase. Measurements were made from 82.5 to 112.5°C., at atmospheric pressure with acetone partial pressures from 30 to 220 mm. Hg., and using radiation in the range 2200 to 3500Å. Most of the work was done using helium as a diluent. By connecting the product stream directly to a gas chromatograph it was possible to use a differential flow reactor in which the conversion did not exceed 2%.

APPARATUS

The reactor and accessories are shown schematically in Figure 1. Helium was split into two separately metered streams, one of which was dispersed in the acetone saturator which was maintained at 24°C., somewhat below room temperature (26°C.) to prevent condensation of acetone following the saturator. Except for the flow controlling apparatus and silica gel dryers of glass, and the quartz reactor, the piping was fabricated of stainless steel tubing.

The elliptical reflector with radiation lamp and tubular reactor at the two foci, was similar to that used originally by Baginsky (*5*). The reflector was made of highly polished aluminum sheet, 0.032 in. thick. The reactor of fused, optically clear quartz, had an I.D. of 20 mm. (23 mm. O.D.) and an irradiated length of 200 mm. Reaction temperature was maintained by passing heated air through a quartz jacket (I.D. = 32 mm.). Axial temperature variations up to 5°C. were measured with a traveling thermocouple in the jacket. The variation was nearly linear, and temperatures quoted refer to values at the midpoint along the reactor length.

A Hanovia LL, 189A10, 1200 W, high pressure, quartz, mercury-vapor lamp was used. The spectrum of energy output in the 2200 to 3500Å. range, as supplied by the manufacturer (*7*), is given in the second column of Table 2. To be able to change the light intensity without altering the spectral distribution, filter solutions were circulated, at controlled temperatures, through three quartz jackets surrounding the lamp. These jackets, not shown separately in Figure 1, were formed by concentric quartz tubes around the lamp. The inside-outside diameters of these tubes were 42 to 45 mm., 57 to 61 mm., 70 to 74 mm., and 85 to 89 mm. Through the space between the lamp and first jacket, room temperature air was passed for cooling. In the first, second, and third jackets (of thickness 6.0, 4.5, and 5.5 mm.) flowed solutions of ferric chloride hydrate (*p*H adjusted to 1.8 with hydrochloric acid), cobaltous sulfate, and nickel sulfate, respectively. Different levels of light intensity at the reactor wall were obtained by varying the concentration of ferric chloride in the first jacket. The concentrations of cobaltous sulfate and nickel sulfate were constant at 0.25 and 1.5 moles/liter, respectively. An initial radiation period was required to obtain a stable transmission coefficient for the solutions and frequent checks on stability were subsequently made by using a Beckman DK-2A spectrophotometer. For filter solutions 1, 2, 3, the concentration of ferric chloride hydrate was 2.46×10^{-4}, 1.23×10^{-4}, and 0 g.mole/liter. Filter solution No. 4 was the same as No. 3, except its transmission was stabilized after a longer initial radiation period.

The product gas from the reactor was divided into two streams and sent through separate sampling devices to two columns of the chromatograph for analysis. Column A contained 20 ft. of molecular sieve 5A, 30-60 mesh, for deter-

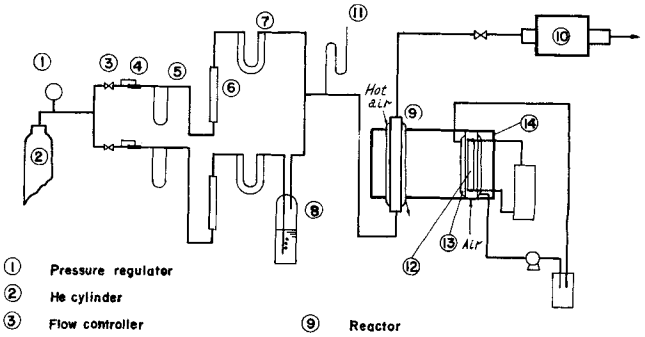

① Pressure regulator
② He cylinder
③ Flow controller
④ Flow regulator
⑤ Capillary flowmeter
⑥ Soap flowmeter
⑦ Silicagel drier
⑧ Acetone saturator
⑨ Reactor
⑩ Gas chromatograph
⑪ Mercury manometer
⑫ High pressure mercury-vapor lamp
⑬ Filter solution jackets
⑭ Elliptical reflector

Fig. 1. Schematic diagram of equipment.

Takeshi Matsurra is on leave from University of Tokyo, Tokyo, Japan. A. E. Cassano is on leave from Facultad de Ingenieria Quimica, Santa Fe, and Consejo de Investigaciones, Argentina.

mination of oxygen, nitrogen, carbon monoxide and methane. Column B consisted of 10 ft. of Porapack Q, 80-100 mesh and was used for carbon dioxide, ethane, biacetyl, and acetone. With proper temperature programming in each column the peak for each component was clearly separated so that accurate area measurements could be obtained. The acetone used was spectrophotometric grade and the helium gas from the cylinder had a stated purity of 99.99%.

TREATMENT OF THE RATE DATA

Reproducibility of the rate measurements was evaluated in a preliminary run carried out over a period of two days at 102.5°C., 100 mm. mercury acetone partial pressure and at a total flow rate of 140 cc./min. (102.5°C., 1 atm.). The products were primarily ethane and carbon monoxide, with a measurable amount of biacetyl. Conversions of acetone into these three products at these operating conditions were 0.46, 0.42, and 0.04%, respectively. The fraction of the acetone converted to biacetyl seemed to be constant at one temperature. Traces of methane and carbon dioxide were detected but their chromatographic peaks were too small to measure.

The rates of carbon monoxide and ethane formation were reproducible to ± 4%, while the results for biacetyl scattered a little more, due to its small magnitude. The overall reactions for producing the three measurable products are:

$$CH_3CO\,CH_3 \rightarrow C_2H_6 + CO \qquad (1)$$

$$2CH_3CO\,CH_3 \rightarrow C_2H_6 + (CH_3\,CO)_2 \qquad (2)$$

The biacetyl produced was always approximately equal to the difference between that of ethane and carbon monoxide as required by the stoichiometry of Equations (1) and (2). The rate $\bar{r}_d$ reported in the following sections is the total rate of decomposition of acetone. It was evaluated from the observed rates of formation of ethane and biacetyl. According to reactions (1) and (2) the relationship is

$$\bar{r}_d = \bar{r}_{C_2H_6} + \bar{r}_{Bi} \qquad (3)$$

It is well known (*1*) that small amounts of oxygen can alter the course of a photochemical reaction, and this has been quantitatively demonstrated in acetone photolysis (*2*). Precautions were taken to prevent leaks in the apparatus. Chromatographic analysis indicated that the oxygen level, before photo-oxidation, did not exceed 30 ppm. This initial concentration was always less than 4% of the acetone reacted. The trace of carbon dioxide observed in the products was probably due to photo-oxidation.

The rates of formation of ethane and $(CH_3CO)_2$ were calculated from the measured concentrations and the flow rate Q, according to the differential reactor expression

$$\bar{r}_i = \frac{Q(C_i - 0)}{V} \qquad (4)$$

The assumption of constant concentration, and therefore constant rate, is justified since the conversion was always less than 2%. In preliminary runs, at 102.5°C. and 100 mm. mercury acetone pressure, the flow rate was changed from 35 to 205 cc./min. (102.5°C., 1 atm.). The rates calculated from Equation (4) were constant (± 3.3% variation), as they should be for differential reactor operation. On subsequent measurements runs were made at flow rates from 130 to 170 cc./min. The flow was always laminar.

In the preliminary work a white deposit was found on the inside of the reactor wall after several runs. It appeared to form more rapidly at low gas velocities. Removal was easily accomplished by brushing after the surface had been wet with acetone. The rate, after cleaning, was the same as in the original clean reactor run. Acetone photolysis is not supposed to involve wall reactions. However, among possible explanations could be impurities in the acetone or a slight amount of photo-oxidation. The reactor was cleaned periodically during the final measurements to ensure no wall effects.

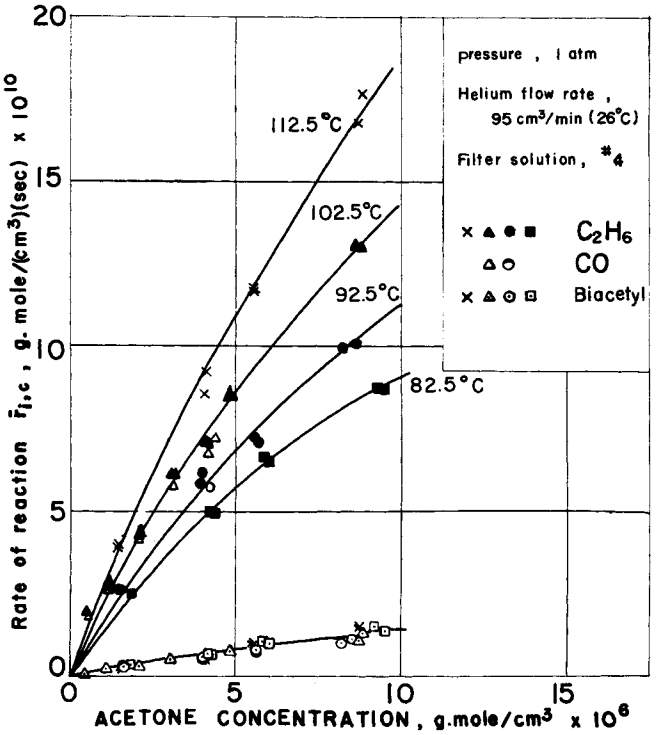

Fig. 2. Reaction rate vs. acetone concentration.

Illustrative results for $\bar{r}_i$ are shown in Figure 2 for various temperatures and acetone concentrations. Filter solution No. 4 was used for these data. Its transmission characteristics are given in Table 2.

ACETONE ABSORPTIVITY

While the effect of temperature on the absorptivity of acetone is thought to be small, the only published data not at room temperature is that of Luckey and Noyes (12). They reported values at various temperatures, but only for monochromatic radiation (at 3130Å). Since our measurements used light from 2,200 to 3,500Å, absorp-

Table 1. Absorptivity of Acetone [l/(g.mole)(cm.)]* at Various Temperatures

λ	Temperature			
Å	25°C.	50°C.	97°C.	105°C.
2,050	2.73	2.73	2.34	2.33
2,150	2.41	2.24	1.76	1.52
2,250	4.06	3.89	3.72	3.15
2,350	11.92	12.11	12.20	12.85
2,450	14.06	14.16	14.44	14.73
2,550	23.48	23.59	23.80	24.77
2,650	31.19	31.66	32.61	33.45
2,750	33.93	34.82	36.15	36.65
2,850	30.95	31.19	33.21	33.69
2,950	22.32	22.74	24.88	25.10
3,050	12.85	13.41	14.92	15.59
3,150	5.80	5.82	7.02	7.02
3,250	3.06	3.48	3.97	4.06
3,350	0.64	0.72	0.93	0.87
3,450	0.55	0.64	0.72	0.79

* Based on log$_e$.

tivities were determined over this range from 25 to 105°C. by measuring the transmittance of helium-acetone mixtures in a Beckmann DK 2A spectrophotometer. By using a saturated mixture of acetone in helium in a 10 cm. silica cell at 25°C., absorptivities were determined vs. λ for this temperature. The results agreed well with the value in the literature at 2,800Å. (*1*). Then a somewhat undersaturated mixture was subjected to transmission measurements in a 5 cm. cell at 25°C. and other temperatures. The previously determined value of α at 25°C. and 2,800Å. was used to evaluate the acetone concentration in this undersaturated mixture. The resultant absorptivities are given in Table 1. At 2,750Å. where α is largest, there is a 7.3% increase between 25 and 105°C. In the temperature range of the kinetic measurements (82.5 to 112.5°C.) the maximum variation is only 2.7%. Consequently the values at 97°C. were used in the subsequent calculations for all temperatures.

ANALYSIS OF DATA

Local Rate Expression

The mechanism of gas phase photolysis of acetone has been studied extensively in photochemical cells and reviews of the literature are available (*4, 16*). The primary and secondary steps are believed to be

Primary reactions:

$$\xrightarrow{k_5 = \phi_5 \alpha_\lambda I_\lambda} \quad \text{CH}_3\text{COCH}_3 + h\nu \rightarrow \text{CH}_3\text{COCH}_3^* \qquad (5)$$

$$\text{CH}_3\text{COCH}_3^* + \text{CH}_3\text{COCH}_3 \xrightarrow{k_6} 2\text{CH}_3\text{COCH}_3 \qquad (6)$$

$$\text{CH}_3\text{COCH}_3^* \xrightarrow{k_7} \text{CH}_3\text{CO}\cdot + \text{CH}_3\cdot \qquad (7)$$

Secondary reactions:

$$\text{CH}_3\text{CO}\cdot + \text{CH}_3\cdot \xrightarrow{k_8} \text{CH}_3\text{COCH}_3 \qquad (8)$$

$$\text{CH}_3\text{CO}\cdot \xrightarrow{k_9} \text{CH}_3\cdot + \text{CO} \qquad (9)$$

$$2\text{CH}_3\cdot \xrightarrow{k_{10}} \text{C}_2\text{H}_6 \qquad (10)$$

$$2\text{CH}_3\text{CO}\cdot \xrightarrow{k_{11}} (\text{CH}_3\text{CO})_2 \qquad (11)$$

Additional free radical reactions may be written particularly for the formation of methane and methyl ethyl ketone, but measurable amounts of these products were not found so only reactions (5) to (11) need be considered. The possibility of a significant lifetime for the activated acetone molecule, and therefore reactions (6) and (7) has been proposed by others (*15*) and indicated by the experimental work of Roebber, Rollefson, and Pimentel (*14*). Our study showed the rate of acetone decomposition to be less than first-order, suggesting reformation of acetone by reactions (6) and (8).

The secondary reactions represent all possible recombinations of the two free radicals, $\text{CH}_3\cdot$ and $\text{CH}_3\text{CO}\cdot$. As mentioned, the available data indicate that wall reactions are not significant at the pressures studied here. The further decomposition of $\text{CH}_3\text{CO}\cdot$ by reaction (9), if it is thermal, has an activation energy of 12 to 15 kcal./mole (*6, 12a*). It is the only reaction mentioned that should have a significant activation energy.

In formulating the rate expression, three assumptions will be made: (a) only those reactions shown are important; (b) the stationary state hypothesis is valid for $\text{CH}_3\text{COCH}_3^*$ for the experimental conditions used; (c) the rates of the secondary reactions are such that the fraction $1 - \delta$, of the molecules decomposed by reaction (7) which return to acetone by reaction (8), is independent of acetone concentration. It has been mentioned that the ratio of biacetyl formation to the total conversion was constant over the acetone partial pressure range studied. This means, if we assume the postulated reactions, that the ratio of the rates of reaction (11) to the sum of (9) and (11) was constant at a fixed temperature. This is the basis for the assumption that the ratio of (8) to (7) is also constant. This ratio will be a function of temperature since reaction (9) is known to have a significant activation energy.

The stationary state hypothesis requires that

$$\frac{d(\text{CH}_3\text{COCH}_3^*)}{dt} = \phi_5 \alpha_\lambda I_\lambda (\text{CH}_3\text{COCH}_3) - k_6 (\text{CH}_3\text{COCH}_3^*)(\text{CH}_3\text{COCH}_3) - k_7 (\text{CH}_3\text{COCH}_3^*) = 0 \qquad (12)$$

Since the quantum yield, ϕ_5, for reaction (5) will be unity, this expression yields

$$(\text{CH}_3\text{COCH}_3^*) = \frac{\alpha_\lambda I_\lambda (\text{CH}_3\text{COCH}_3)}{k_6(\text{CH}_3\text{COCH}_3) + k_7} \qquad (13)$$

The total decomposition rate of acetone is given by

$$\frac{-d(\text{CH}_3\text{COCH}_3)}{dt} = k_7 \delta(\text{CH}_3\text{COCH}_3^*) \qquad (14)$$

With Equation (13) this may be written

$$\frac{-d(\text{CH}_3\text{COCH}_3)}{dt} = r_{d,\lambda} = \frac{\delta \alpha_\lambda I_\lambda (\text{CH}_3\text{COCH}_3)}{1 + \frac{k_6}{k_7}(\text{CH}_3\text{COCH}_3)} \qquad (15)$$

The experimental measurements, through Equations (3) and (4) gave an average rate, $\overline{r_d}$, over the entire reactor and for polychromatic light. Equation (15) can be tested once the relationship between the local rate, for radiation of wave length, λ, and $\overline{r_d}$ is established. This relationship should take into account, among other things, the variation in intensity with radial position in the reactor and the effects of wave length. These are treated in the next

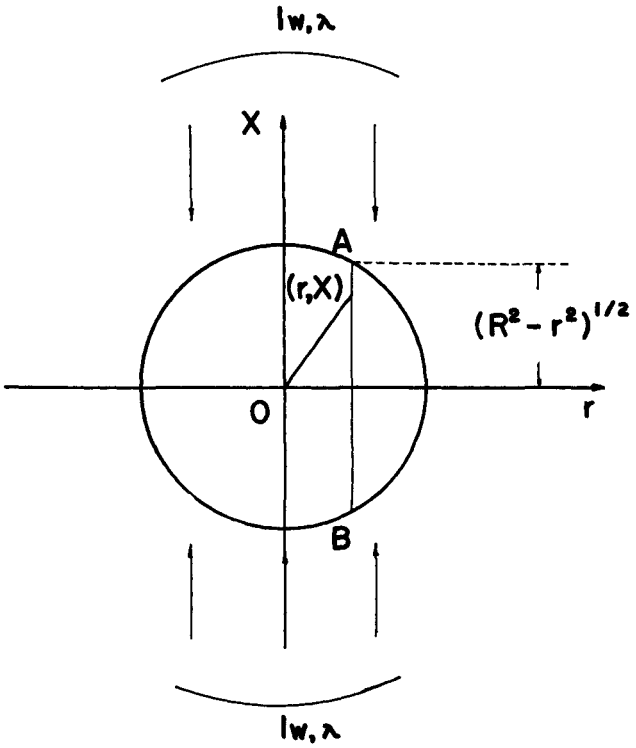

Fig. 1a. Photoreactor geometry.

section.

Relationship between Local and Average Rates

The variations of intensity and absorptivity with wave length should be accounted for in applying Equation (15) to polychromatic light. The rate constants for the secondary reactions (6) and (7) and also δ should be independent of wave length and will be so treated. Hence the local rate summed over all wave lengths will be

$$r_d = \frac{\delta C_A}{1 + \frac{k_6}{k_7} C_A} \sum_\lambda \alpha_\lambda I_\lambda \qquad (16)$$

where C_A represents the acetone concentration. The local intensity, I_λ, also varies with position across the radius of the reactor because of the finite absorptivity of acetone (it will be assumed that the intensity is constant in the axial direction). If the reflector were an exact ellipse and the lamp and reactor were located exactly at the foci, and the lamp was a line source, the distribution of intensity within the reactor could be calculated assuming that the radiation was radially incident to the reactor tube. In the real reactor system shown in Figure 1 it seems more appropriate to suppose a diffuse light pattern; that is light of uniform intensity strikes the reactor from any one direction across the whole diameter of the tube (Figure 1*a*). In addition it is supposed that there is equal probability of the light striking the reactor from any direction. By using these concepts the average intensity, $\overline{I}_\lambda$, (due to radiation from opposite rays in one direction) in the reactor can be related to the intensity reaching the reactor wall from the lamp, $I_{w,\lambda}$, the absorptivity of acetone, and the radius of the reactor. The result, which is derived in the Appendix is

$$\overline{I}_\lambda = 2I_{w\lambda}\left[1 - \frac{4}{3\pi}(\alpha_\lambda C_A R) + \frac{1}{2!}(\alpha_\lambda C_A R)^2 - \ldots\ldots\right] \qquad (17)$$

the local rate in Equation (16) can be converted to the average rate across the reactor diameter by replacing I_λ with $\overline{I}_\lambda$. This is valid because the other quantities in Equation (16) do not vary with radial position; C_A is constant because the reactor operates differentially. Hence, the average rate is obtained by combining Equations (16) and (17):

$$\overline{r}_d = \frac{2\,\delta C_A}{1 + \frac{k_6}{k_7} C_A} \sum_\lambda \alpha_\lambda I_{w,\lambda}\left[1 - \frac{4}{3\pi}(\alpha_\lambda C_A R) + \frac{1}{2!}(\alpha_\lambda C_A R)^2 - \ldots\right] \qquad (18)$$

To treat the diminution of intensity by the use of filter solutions, a hypothetical intensity, $I_{b,\lambda}$, is introduced. This is the intensity which would exist at the reactor wall if no filter solutions were employed. The total intensity for all wave lengths $I_{b,\,tot}$, is related to $I_{b,\lambda}$ by the normalized energy output of the lamp, $F_{\lambda/F_{tot}}$, (given in Table 2) as follows:

$$I_{b,\lambda} = I_{b,tot}\left(\frac{F_\lambda}{F_{tot}}\right) \qquad (19)$$

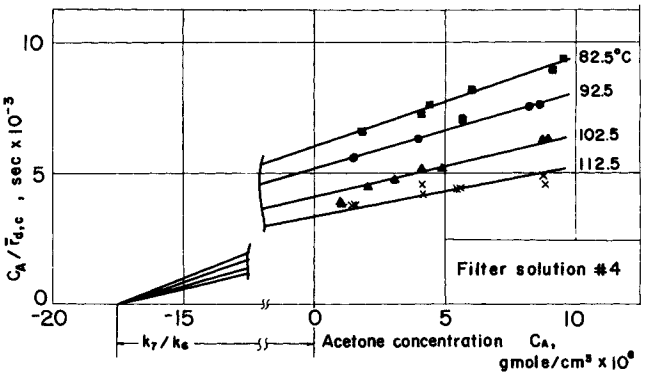

Fig. 3. Correlation of rate data.

If T_λ is the transmission of the filter solutions then

$$I_{w,\lambda} = I_{b,tot}\frac{F_\lambda}{F_{tot}} T_\lambda \qquad (20)$$

Since $I_{b,tot}$ is independent of wave length, Equation (18) may be written

$$\overline{r}_d = \frac{2C_A\,\delta\, I_{b,tot}}{1 + \frac{k_6}{k_7} C_A} \sum_\lambda \frac{F_\lambda}{F_{tot}} T_\lambda \alpha_\lambda \left[1 - \frac{4}{3\pi}(\alpha_\lambda C_A R) + \frac{1}{2!}(\alpha_\lambda C_A R)^2 - \ldots\right] \qquad (21)$$

It is convenient to use a corrected rate $\overline{r}_{d,c}$ which would be applicable if acetone had zero absorptivity, as far as the effect on diminishing the intensity is concerned. Then from Equation (17) we obtain

$$\overline{I}_\lambda = 2I_{w,\lambda};\ \ (\text{for } \alpha_\lambda C_A \to 0) \qquad (22)$$

and Equation (21) becomes

$$\overline{r}_{d,c} = \frac{2C_A(\delta\, I_{b,tot})}{1 + \frac{k_6}{k_7} C_A} \sum_\lambda \frac{F_\lambda}{F_{tot}} T_\lambda \alpha_\lambda \qquad (23)$$

If a correction factor, f, is defined so that

$$\overline{r}_{d,c} = f\,\overline{r}_d \qquad (24)$$

then

$$f = \frac{\sum_\lambda \frac{F_\lambda}{F_{tot}} T_\lambda \alpha_\lambda}{\sum_\lambda \frac{F_\lambda}{F_{tot}} T_\lambda \alpha_\lambda \left[1 - \frac{4}{3\pi}(\alpha_\lambda C_A R) + \frac{1}{2!}(\alpha_\lambda C_A R)^2 - \ldots\right]} \qquad (25)$$

In analyzing the data the procedure followed was to multiply the experimentally derived $\overline{r}_d$ by f to obtain $\overline{r}_{d,c}$, and then to evaluate the kinetic constants through the use of Equation (23). The correction factor is a slight function of concentration of acetone [Equation (25)]. By using the information in Table 2,* f was evaluated for various C_A, and the results are given in Table 3. It should

Table 3. Correction Factor for Finite Absorptivity in Reactor

$C_A \times 10^3$ g.moles/(l)	f
2.0	1.020
4.0	1.038
6.0	1.053
8.0	1.068
10.0	1.080

* Table 2 has been deposited as document NAPS-00373 with the ASIS National Auxiliary Publications Service, c/o CCM Information Sciences, microfiche or $3.00 for photocopies.

be noted that the question of diffuse vs. radial incident light has no effect on the kinetics of the reaction. The use of radial incident light would still give a rate equation first-order in $I_{b,tot}$ like Equation (21). What would change is the form of the term in brackets in the summation. This would mean that the absolute value of $I_{b,tot}$, determined by kinetic studies through equations like (21), would depend upon the form in brackets. Since δ cannot be evaluated independently, only the product $\delta I_{b,tot}$ can be established. Hence, whether the radiation was radially incident or diffuse is not of significance in this work.

Evaluation of $\delta I_{b,tot}$

Equation (23), when rearranged to

$$\frac{C_A}{\overline{r_{d,c}}} = \frac{1}{2(\delta I_{b,tot}) \sum_\lambda \frac{F_\lambda}{F_{tot}} T_\lambda \alpha_\lambda} + \frac{(k_6/k_7) C_A}{2(\delta I_{b,tot}) \sum_\lambda \frac{F_\lambda}{F_{tot}} T_\lambda \alpha_\lambda} \quad (26)$$

suggests that a plot of $C_A/\overline{r_{d,c}}$ vs. C_A should be linear. The data of Figure 2 (for Filter solution No. 4) are so plotted in Figure 3, and agree with the straight line relationship. All the quantities in the expression for the intercept are known except $\delta I_{b,tot}$ and are tabulated in Table 2. The transmission T_λ of the system of three filter solutions was evaluated from the measured absorptivity of each separate solution. The summation $\sum_\lambda (F_\lambda/F_{tot}) T_\lambda \alpha_\lambda$ is given at the bottom of Table 2 for each series of filter solutions 1 to 4. These values and the intercepts in plots such as Figure 3 are sufficient to calculate $(\delta I_{b,tot})$.

From $\delta I_{b,tot}$ the actual intensity function at the reactor wall with filter solutions could be calculated as follows:

$$\delta I_{w,tot} = \delta I_{b,tot} \sum \frac{F_\lambda}{F_{tot}} T_\lambda \quad (27)$$

Evaluation of Rate Constants

$\delta I_{b,tot}$ determined as just described is given in Table 4 for each temperature. From the slopes of the lines in Figure 3 and $\delta I_{b,tot}$ the ratio k_6/k_7 of kinetic constants can be obtained, and these values are also shown in Table 4.

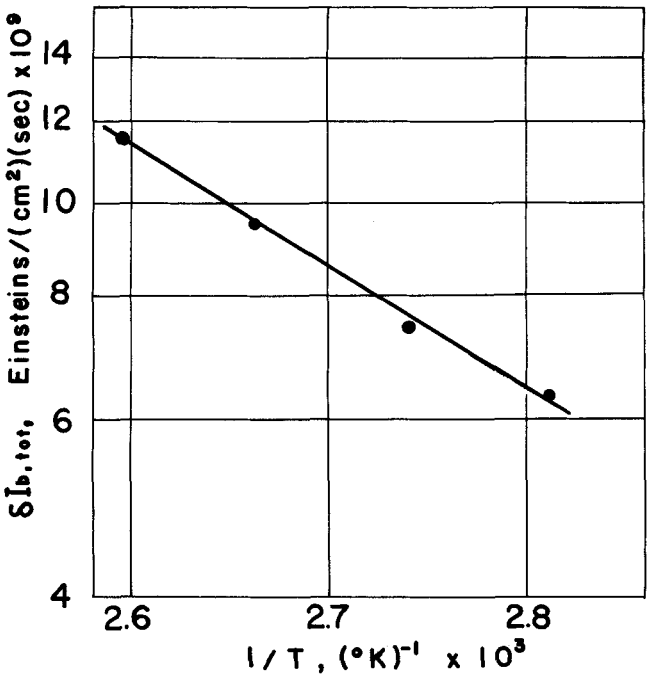

Fig. 4. Arrhenius plot for $\delta I_{b,tot}$.

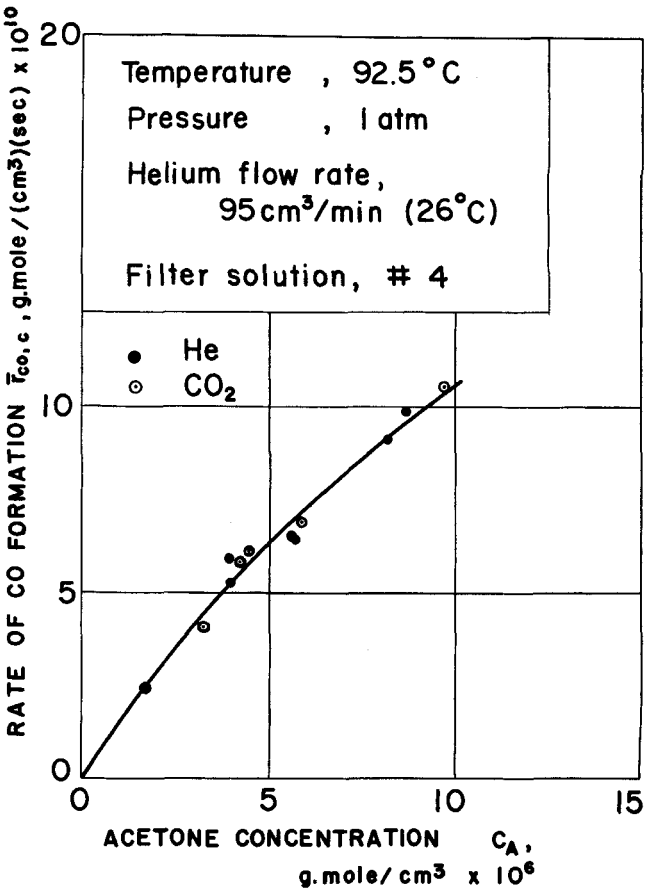

Fig. 5. Effect of diluent upon rate of carbon monoxide formation.

TABLE 4. COEFFICIENTS OF RATE EQUATION (26)

Temperature °C.	$(\delta I_{b,tot}) \times 10^8$ Einsteins/(sq.cm.)(sec.)	k_6/k_7 l/g. mole
82.5	0.641	57.2
92.5	0.743	57.2
102.5	0.938	57.2
112.5	1.145	57.2

The variation of $\delta I_{b,tot}$ with temperature measures the effect of temperature on δ since $I_{b,tot}$ is constant. While there is no theoretical justification, the temperature effect, for comparison purposes, can be expressed in the Arrhenius form. The results are so plotted in Figure 4 and suggest an equivalent activation energy of 4.7 k.cal./g.mole. From the postulates about the mechanism, δ is the ratio of the rates of reactions (9) + (11) to (7). As mentioned, reaction (9) has an activation energy of 12 to 15 k.cal., while (7) and (11) are essentially independent of temperature. Hence, the variation of δ with temperature would be expected to be less than corresponding to E = 12 to 15 k.cal. From this standpoint the observed value of 4.7 k.cal. is not unreasonable.

Figure 3 shows that the lines for different temperatures converge approximately at a single point on the abscissa. This means that k_7/k_6 is independent of temperature, and equal to the intercept on the abscissa. Rate constant k_7 is for the destruction of the activated acetone molecule and is independent of temperature. Reaction (6) represents the deactivation of $CH_3COCH_3^*$ by collision with an acetone molecule of lower energy. Its rate will be proportional to the number of collisions between $CH_3COCH_3^*$ and CH_3COCH_3. The collision number has a temperature coefficient $T^{1/2}$, which is small in comparison with a significant activation energy. Hence, k_6 should be nearly independent of temperature. It is not unexpected that k_7/k_6 would be constant as indicated in Figure 3.

Effect of Diluent

The primary and secondary reactions (5) to (11) do not involve diluent molecules. Hence no effect would be expected if the diluent gas were changed to another species, as long as it were relatively inert. To verify this, runs were made using carbon dioxide in place of helium. Rates were the same as when helium was used, as shown in Figure 5 where the corrected rate of formation of carbon monoxide is plotted vs. C_A.

Effect of Light Intensity

The postulated rate equation, Equation (18), requires that $\bar{r}_d$ be directly proportional to the light intensity at the wall of the reactor, $I_{w,\lambda}$. The output of the lamp could not be varied, so the effect of light intensity was studied by measuring reaction rates with a different concentration of ferric chloride hydrate in the first jacket that is, by using a different transmission level for the filter solutions around the lamp. With this operating procedure the intensity at the wall is measured by the values of the summation in Equation (23). The transmission characteristics of each solution are given in Figure 6. In preparing the different solutions an attempt was made to obtain the same special distribution so as to measure only the effect of intensity level. From the curves in Figure 6, $\Sigma(F_\lambda/F_{tot})T_\lambda\alpha_\lambda$ was calculated and the resulting values are shown in the figure.

The rate data were plotted as in Figure 3, obtaining a separate straight line for each filter solution. The intercepts of these lines at $C_A = 0$ are seen from Equation (26) to give values of $2(\delta I_{b,tot})\ \Sigma(F_\lambda/F_{tot})T_\lambda\alpha_\lambda$. From Equation (23), these values are also equal to

$$\frac{\bar{r}_{d,c}[1 + (k_6/k_7)C_A]}{C_A}$$

and should be directly proportional to $\Sigma(F_\lambda/F_{tot})T_\lambda\alpha_\lambda$. The results, shown in Figure 7, follow a linear relationship passing through the origin. This indicates that the first-order dependency of the rate on $I_{w,\lambda}$, suggested by the mechanism, is followed.

DISCUSSION

Equation (23) fits the rate data over the range of operating conditions, and the values of the kinetic constants appear reasonable. The nonlinear effect of concentration was verified in some preliminary measurements made to evaluate the performance of a batch recycle photoreactor (2).

We found it necessary to introduce the ratio, δ, to treat the complex kinetics involved. This meant that only $\delta I_{b,tot}$, and not the intensity itself, could be evaluated from the rate data. The photolysis of acetone has been mentioned as a gaseous actinometer (8), but our results show that this would not be possible at the conditions studied.

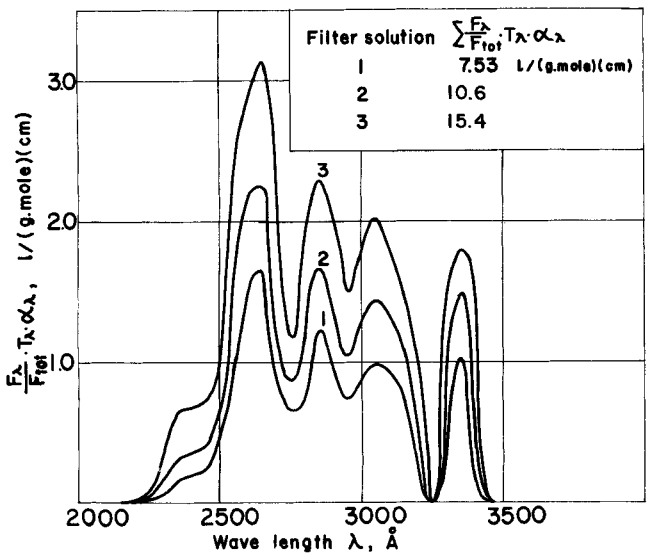

Fig. 6. Characteristics of filter solutions.

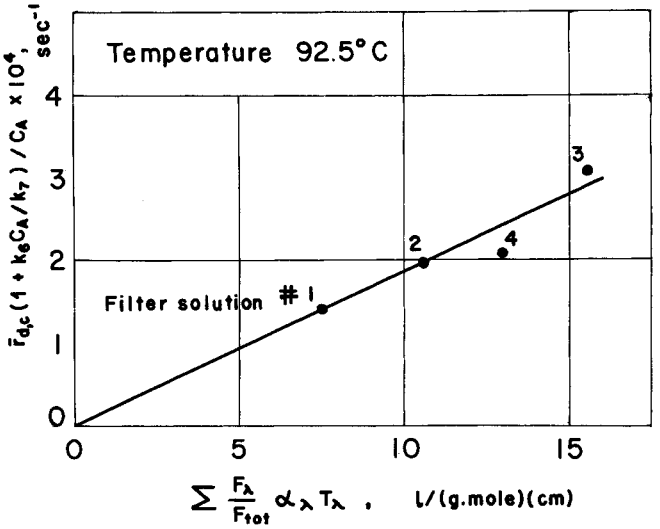

Fig. 7. Effect of light intensity on rate.

The numbers in Table 4 show that δ increases with temperature. It is expected that δ would approach unity as the temperature rises since the free radical recombination into acetone by reaction (8) would become relatively less important with respect to destruction of $CH_3CO\cdot$ [by reaction (9)]. The data in Table 4 do not suggest that this point is reached at 112.5°C. However, the value of $\delta I_{b,tot}$ at this temperature gives a minimum figure for the intensity. It might be possible to use acetone photolysis as a means of measuring the intensity, if operating temperatures could be increased. This would require a higher temperature fluid in the jacket which would have stable transmission coefficients in the range 2000-3600Å. Also operation at acetone partial pressures less than 50 mm. would reduce the significance of reaction (6). It has been mentioned (8) that at 150°C. and low acetone partial pressures only reactions (5), (7), (9), and (10) would occur. Under these conditions the quantum yield of carbon monoxide would be unity. In our study ϕ_{CO} was considerably less than one, because of the reformation of stable acetone molecules.

ACKNOWLEDGMENT

The financial support of the Federal Water Pollution Control Administration through Grant WP 00952 is gratefully acknowledged.

NOTATION

- C_i = concentration of species i at reactor temperature and pressure, g.moles/cc.
- f = correction factor defined by Equation (25)
- F_λ = energy output of lamp at wave length, λ, Einsteins/sec.
- I_λ = light intensity at wave length, λ, Einsteins/(sq. cm.)(sec.)
- $\bar{I}_\lambda$ = average light intensity over reactor cross section
- I_b = light intensity which would exist at reactor wall if no filter solutions were used
- I_w = light intensity at reactor wall with filter solutions
- k_n = reaction rate constant for elementary reaction of number n with appropriate cm. g. sec. units
- Q = volumetric flow rate at reactor conditions, cc./sec.
- R = radius of reactor, cm.

r_i = total rate of formation of product i; that is, rate summed for all wave lengths, g.moles/(cc.)(sec.)
r_d = total rate of decomposition of acetone, g.moles/(cc.)(sec.)
$\bar{r}_d$ = average, total rate over reactor cross section
$\bar{r}_{d,c}$ = $f\,\bar{r}_d$
T_λ = fraction of light of wave length, λ, transmitted through all filter solutions
V = irradiated volume of reactor, cc.
α_λ = absorptivity of acetone; in tables units are 1/(g.moles)(cm.); in equations sq. cm./(g.mole) is used. All values based upon intensity ratio in $\log_e$ form
δ = ratio of rate of products formation to total rate of decomposition of activated acetone molecules
λ = wave length, Å. or cm.
ϕ_i = quantum yield of product or reaction i, g.moles/Einstein
( ) = denotes concentration, g.moles/cc.
tot = total for all wave lengths

LITERATURE CITED

1. Calvert, J. G., and J. N. Pitts, Jr., "Photochemistry," John Wiley, New York (1966).
2. Cassano, A. E., T. Matsuura, and J. M. Smith, *Ind. Eng. Chem. Fundamentals*, **7**, 655 (1968).
3. ———, and J. M. Smith, *AIChE J.*, **12**, 1124 (1966); **13**, 915 (1967).
4. Davis, W., Jr., *Chem. Rev.*, **40**, 201 (1947).
5. Baginsky, I. C., D. Eng. dissertation, Yale Univ., New Haven, Conn. (1951).
6. Gorin, E., *J. Chem. Phys*, **7**, 256 (1936).
7. Hanovia High-Pressure Quartz Mercury-Vapor Lamp Spectral Energy Distribution, Bull. EH-223.
8. Herr, D. S., and W. A. Noyes, Jr., *J. Amer. Chem. Soc.*, **62**, 2052 (1940).
9. Huff, J. E. and C. A. Walker, *AIChE J.*, **8**, 113 (1962).
10. Harris, P. R. and J. S. Dranoff, *ibid.*, **11**, 497 (1965).
11. Jacob, S. M., and J. S. Dranoff, *Chem. Eng. Prog. Symp. Ser.*, **62**, 47 (1966).
12. Luckey, G. W. and W. A. Noyes, Jr., *J. Chem. Phys.*, **19**, 227 (1951).
13. O'Neale, E. and S. Benson, *ibid.*, **36**, 2196 (1962).
14. Roebber, J. L., G. K. Rollefson, and G. C. Primentel, *J. Amer. Chem. Soc.*, **80**, 255 (1958).
15. Spence R. and W. Wild, *J. Chem Soc.*, 352 (1937); 590 (1941).
16. Steacie, E. W. R., "Atomic and Free Radical Reactions," Vol. I and II, Reinhold, New York (1954).

Manuscript received February 2, 1968; revision received April 26, 1968; paper accepted April 29, 1968.

APPENDIX

If a diffuse light pattern is assumed, radiation of uniform intensity, $I_{w,\lambda}$, will strike the reactor at any position across the diameter, as shown in Figure 1A. Further there will be equal probability of the light coming from any direction. It is sufficient, in this situation, to calculate the average light intensity over the cross-sectional area of the reactor by considering light from a single direction, as shown in the figure. This is true because the ratio of the average intensity for finite and zero absorptivities of acetone is the same whether calculated for light from a single direction or from all directions. In the calculations of $r_{d,c}$ from the data, only the ratio f is used, not the absolute intensity $\bar{I}$.

The attenuation of the light as it passes along any ray through the reactor, for example along AB, is determined by Lambert-Beer's law

$$\frac{dI_\lambda}{dx} = \mp \alpha_\lambda C_A I_\lambda \qquad (1A)$$

The total intensity at any point r, x is obtained by integrating Equation (1A) from the reactor wall to r, x in both directions along AB. The result is

$$I_\lambda(r,x) = I_{w,\lambda}\,[\exp\{-\alpha_\lambda C_A[(R^2-r^2)^{1/2}+x]\} + \exp\{-\alpha_\lambda C_A[(R^2-r^2)^{1/2}-x]\}] \qquad (2A)$$

The average intensity over the cross-sectional area is

$$\overline{I_\lambda} = \frac{I_{w,\lambda}}{\pi R^2}\int_{-R}^{R}\int_{-(R^2-x^2)^{1/2}}^{(R^2-x^2)^{1/2}} [\exp\{-\alpha_\lambda C_A[(R^2-r^2)^{1/2}+x]\} + \exp\{-\alpha_\lambda C_A[(R^2-r^2)^{1/2}-x]\}]\,dx\,dr \qquad (3A)$$

If a Taylor series expansion is used for the exponential terms, the integrated result is Equation (17).

Profiles of Laser-Created Cavities on Metal Surfaces

JOHN L. DEMING, JAMES H. WEBER, and LUH C. TAO

University of Nebraska, Lincoln, Nebraska

Metal surfaces of titanium, aluminum, copper, lead, and zinc were irradiated by a 25 joules pulsed laser with an energy flux ranging from 10^6 to 10^8 cal./(sq.cm.) (sec.). The resulted cavities were sectioned, polished and measured to compare with the isotherms computed from several heat conduction models. Reasonable agreement was found between the experimental cavity diameters at the interface and those calculated from the disk source model. Also, a graphical correlation between the cavity depth and its interface diameter is presented.

Laser beams are characterized by their high energy intensity, spatial and temporal coherence, and collimation. Among their many interesting applications are welding and drilling refractory materials and initiating exothermic chemical reactions. All involve the transport of an extremely high energy flux. Lindhom, Baker, Kirkpatrick (*8*) experimented with an electric arc source with a flux of 100 to 1,000 cal./(sq.cm.)(sec.) and found that the conventional theory of heat conduction is valid. The flux in this work is in the order of 10^9 to 10^8 cal./(sq. cm.)(sec.).

Bahun and Engquist (*2*) utilized the conventional heat transfer theory of point source to interpret the melting and vaporization of materials by the energy of a laser beam. Schmidt, Ham, and Hoshi (*10*) made micro hardness tests for the affected area of a metal irradiated by a focused laser beam. Anderson and Jackson (*1*) used the point source solution to illustrate the theory of welding. Ready (*9*) found by high speed photography that a plume of vaporized material started near the end of a laser pulse and that the measured vapor velocities of 2 to 5 $\times$ 10^4 cm./sec. were typical of materials from a boiling surface.

There have been no investigations on the profiles of laser-created cavities. This paper presents the results of